ORGANOMETALLICS

pubs.acs.org/Organometallics Article

Synthesis, Characterization, and Antimicrobial Activity of Rh^{III} and Ir^{III} N-Heterocyclic Carbene Piano-Stool Complexes

Chad M. Bernier, Christine M. DuChane, Justin S. Martinez, Joseph O. Falkinham, III, and Joseph S. Merola*

Cite This: *Organometallics* 2021, 40, 1670–1681 Read Online

ACCESS | Metrics & More | Article Recommendations | Supporting Information

ABSTRACT: A series of Rh^{III} and Ir^{III} piano-stool complexes of the form $[(\eta^5\text{-}Cp^{*R})M(NHC)Cl_2]$ was synthesized and characterized, including 12 X-ray crystallographic structures. The antimicrobial properties of these complexes were screened against a variety of microbes, with several achieving high activities, most notably against *Mycobacterium smegmatis* (MICs as low as 0.45 μM). In general, the Rh complexes were more potent than their Ir analogues, and activity increased with the hydrophobicity of the Cp^{*R} and NHC ligands.

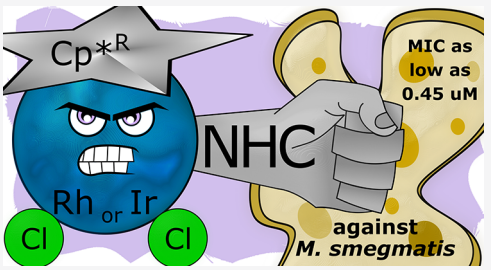

INTRODUCTION

In 2010, the World Health Organization declared antimicrobial resistance to be one of the greatest emerging threats facing humanity, yet relatively little progress has been made in the past decade to develop new classes of antimicrobials, such as metallodrugs.[1] The innate structural diversity of transition-metal complexes makes metallodrugs valuable potential contributors to combat antimicrobial resistance, and investigation into their biological properties has recently been increasing.[2] Transition-metal complexes offer unique, easily modified scaffolds that can accommodate a wide range of ligands and oxidation states, which subsequently affect the stability, bioavailability, lipophilicity, biological target, and many other factors that ultimately contribute to metal-specific mechanisms of action that are virtually unattainable with traditional organic pharmaceuticals. Several excellent review articles have recently been published that illustrate the quickly growing importance of metal-based antimicrobial agents.[3]

Though they have been relatively understudied in comparison to other noble metals such as ruthenium,[4] palladium,[5] silver,[6] platinum,[7] and gold,[8] recent reports have highlighted the promising biological properties of rhodium and iridium piano-stool complexes, particularly those featuring pentamethylcyclopentadienyl (Cp*) and derivatized tetramethylcyclopentadienyl (Cp^{*R}) ligands.[9] Rhodium and iridium piano-stool complexes of this type make intriguing antimicrobial candidates due to their good water solubility and facile modularity, which allows easy modification to tailor the compounds toward specific biological applications and targets (Figure 1).[10]

A myriad of organic ligands have been employed to investigate the biological properties of rhodium and iridium piano-stool complexes, primarily for anticancer applications.[11]

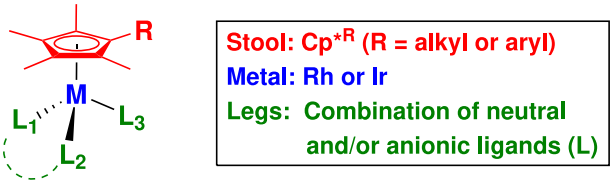

Figure 1. Generic structure of a rhodium or iridium Cp^{*R} piano-stool complex.

Previous reports have indicated that the mechanism of drug action of these complexes is often dependent upon the nature of the ligands coordinated to the metal center, with some complexes having a high affinity for binding to DNA, RNA, and mitochondria, ultimately leading to apoptosis, while others can disrupt the redox balance inside cells.[12] However, many of these processes are still not well-understood for noble-metal complexes, and this continues to be an active area of research.

The rapid development of metallodrugs over the last few decades has led to a growing interest in the biological applications of N-heterocyclic carbene ligands (NHCs), primarily due to their synthetic accessibility and strong σ-donor properties, which typically gives rise to exceptionally stable noble-metal complexes.[13] Silver and gold NHC complexes have been studied extensively for their antimicrobial and anticancer properties, with the activities of some rivaling

Received: March 18, 2021
Published: May 28, 2021

https://doi.org/10.1021/acs.organomet.1c00166
Organometallics 2021, 40, 1670–1681

those of other commonly employed metal-based drugs such as silver sulfadiazine and cisplatin (Figure 2).[14] Several rhodium

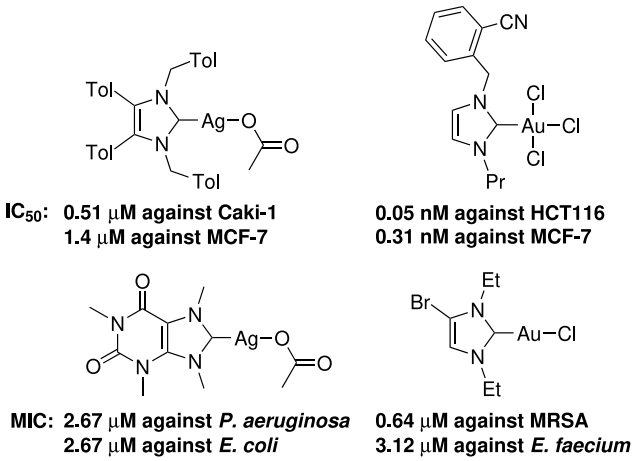

Figure 2. A few examples of silver and gold NHC complexes displaying anticancer (top) and antimicrobial (bottom) activity.[16]

and iridium NHC complexes have also been reported to have anticancer activity, including piano-stool variants featuring Cp* and Cp*^{R} ligands. The cytoxicity is generally enhanced in these piano-stool complexes upon incorporation of hydrophobic substituents into Cp*^{R}, which likely arises from increased cellular uptake of the complexes.[15]

Despite the promising anticancer activity of rhodium and iridium NHC complexes, there have been significantly fewer studies into their antimicrobial properties. Previously reported rhodium and iridium NHC complexes displaying antimicrobial activity against various microbes are provided in Figure 3. The activity is often sensitive to changes in the NHC scaffold and N-substituents. While many of these complexes showed poor activity, investigations have largely focused on Rh^{I} or Ir^{I} square-planar complexes, leaving the realm of Rh^{III} and Ir^{III} NHC piano-stool antimicrobial agents relatively unexplored.

The Merola group has previously highlighted the antimicrobial properties of a series of Rh^{III} and Ir^{III} Cp*^{R} piano-stool complexes featuring a variety of amino acid (17 μM against *M. smegmatis* and *M. bovis*),[18] diamine (9.8 μM against *S. aureus*; 15 μM against MRSA),[19] and β-diketonato (2.2 μM against *M. smegmatis*)[20] ligands (Figure 4, top). Investigations into the cytotoxicity of the iridium Cp* diamine complexes were encouraging, with no toxicity observed against Vero or human embryonic kidney cell lines at concentrations at least 50 times higher than that of the minimum inhibitory concentrations. Additional *in vivo* toxicity screenings on a group of adult outbred white mice showed no detrimental side effects 14 days after administering a single IV dose (2.5 or 5 μg/kg), and a subsequent ICP-OES analysis found practically no iridium in the blood, heart, or lungs of the mice, with most of the iridium localized in the kidneys or excreted as urine.[21]

In order to advance the rapidly growing interest in the biological properties of metal NHC complexes, in this article we report the synthesis, characterization, and antimicrobial activities of Rh^{III} and Ir^{III} piano-stool complexes featuring a series of Cp*^{R} and NHC ligands (Figure 4, bottom). Since the antimicrobial properties of these particular complexes have been understudied up to this point, this work features a wide scope of Cp*^{R} substituents and NHC ligands to further the understanding of structure–activity relationships across noble-metal piano-stool complexes.

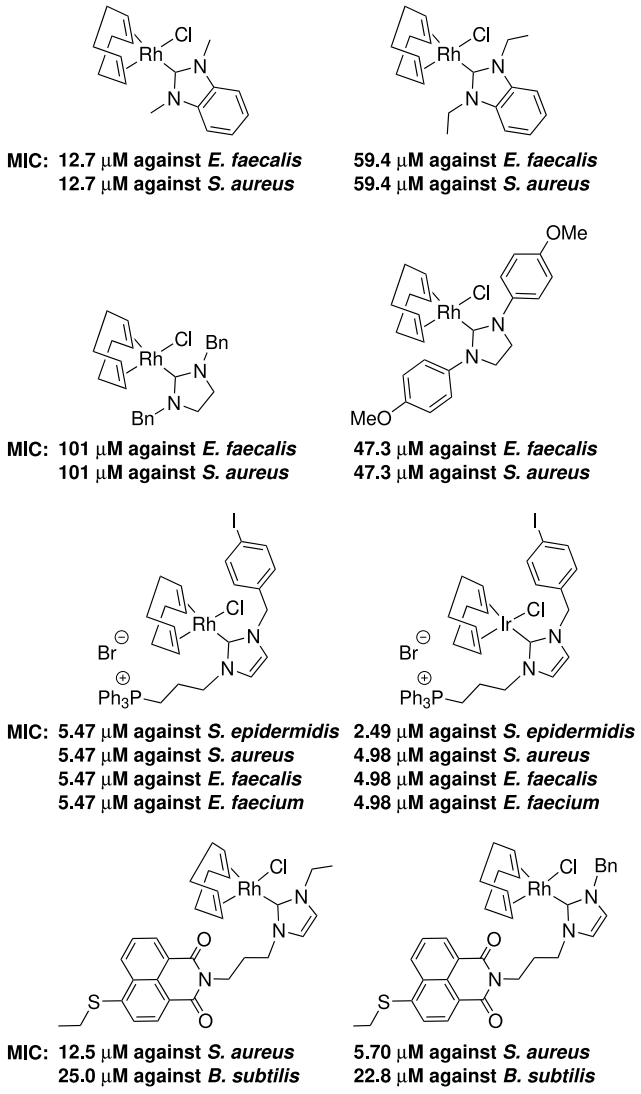

Figure 3. Examples of previously reported rhodium and iridium NHC complexes displaying antimicrobial activity.[17]

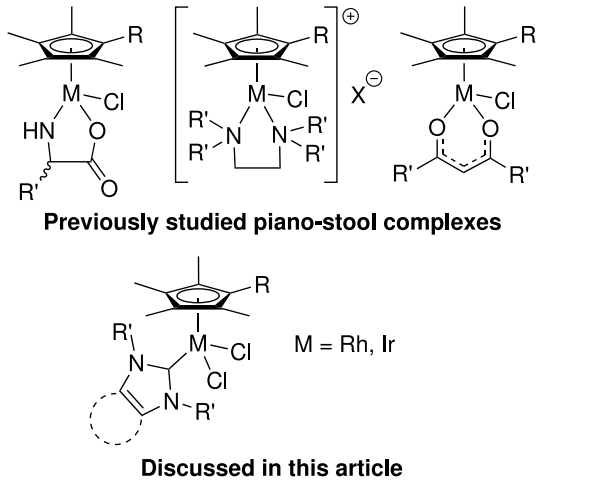

Figure 4. Piano-stool complexes investigated for antimicrobial activity by the Merola group.

https://doi.org/10.1021/acs.organomet.1c00166
Organometallics 2021, 40, 1670–1681

RESULTS AND DISCUSSION

Synthesis and Characterization. $(Cp^{*R})M(NHC)Cl_2$ complexes were synthesized using a modified literature procedure (Scheme 1).[22,23] Silver(I) oxide was added to a

Scheme 1. Synthetic Route to Rh^{III} and Ir^{III} Cp^{*R} NHC Piano-Stool Complexes

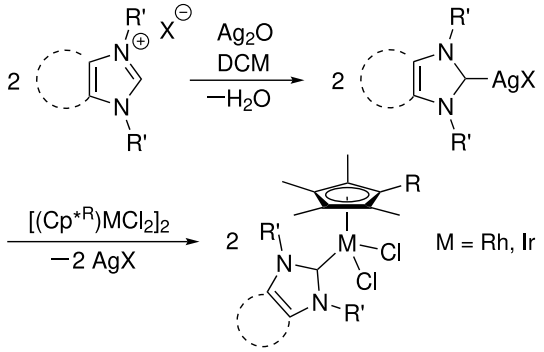

stirring dichloromethane solution of the desired imidazolium salt, and the mixture was allowed to react in the dark at room temperature over a period of 4 h. The appropriate rhodium or iridium Cp^{*R} dimer was then added directly to the reaction flask and stirred at room temperature while the mixture slowly changed from gray to dark red (Rh) or dark yellow (Ir). After 12 h, the crude suspension was filtered and the solvent removed under vacuum. Recrystallization from dichloromethane and hexanes gave rise to the desired products as red (Rh) or yellow (Ir) solids in variable (28−80%) yields (Table 1).

Table 1. Labeling and Yields of Complexes[a]

Cp^{*R}	NHC	Rh complex	yield (%)	Ir complex	yield (%)
methyl	IMe	**Rh-1**[22]	89	**Ir-1**[23]	75
	IEt	**Rh-2**	80	**Ir-2**[24]	68
	I^{i}Pr	**Rh-3**	57		
	ICy	**Rh-4**	75	**Ir-4**[25]	49
	Me_2-bimy	**Rh-5**[15a]	87	**Ir-5**[26]	82
ethyl	IMe			**Ir-6**	69
n-propyl		**Rh-7**	60	**Ir-7**	28
isopropyl		**Rh-8**	59		
n-pentyl		**Rh-9**	45		
n-octyl				**Ir-10**	50
phenyl	IMe	**Rh-11**	78	**Ir-11**	80
	Me_2-bimy	**Rh-12**	48		
benzyl	IMe			**Ir-13**	71
phenethyl		**Rh-14**	73	**Ir-14**	67
C_6F_5		**Rh-15**	31	**Ir-15**	77

[a]References for previously reported complexes are provided next to the labels.

Of the 23 complexes synthesized in this study, 17 are novel, with the exception of **Rh-1**, **Rh-5**, **Ir-1**, **Ir-2**, **Ir-4**, and **Ir-5**. References for previously reported complexes are provided next to the respective labels in Table 1. Characterization included ^{1}H NMR, ^{13}C NMR, high-resolution mass spectroscopy, and single-crystal X-ray diffraction, when possible.

NMR Spectroscopy. The ^{1}H NMR spectra of complexes featuring underivatized Cp* moieties contain a singlet in the range of 1.55−1.70 ppm corresponding to the five equivalent methyl groups on the ring. This equivalence is lost upon incorporation of various alkyl or aryl R groups onto the Cp^{*R} moiety, giving rise to a pair of singlets attributed to the chemically nonequivalent methyl groups along the mirror plane of the ring. For the novel piano-stool NHC complexes reported in this article, these two singlets are typically observed in the range of 1.30−1.80 ppm, depending on the identity of the R substituent.

Coordination of the NHC ligand to the metal center was confirmed via observation of the characteristic downfield resonance of the carbene carbon in the ^{13}C NMR spectra, which was typically found to resonate in the narrow ranges of 166−169 ppm (rhodium complexes) and 152−156 ppm (iridium complexes). The only exception to this is observed for Me_2-bimy, which resonates significantly farther downfield in comparison to the other NHC ligands employed in this work. The carbene carbon resonance in rhodium complexes was observed as the expected doublet due to coupling between the rhodium metal center and the carbene carbon. The values of the $^1J_{Rh-C}$ coupling constants were found to range from 55 to 57 Hz and slightly decrease in relation to the $^1J_{Rh-C}$ value of **Rh-1** upon incorporation of alkyl or aryl R groups into the Cp^{*R} ring. Since the ^{13}C spectral features of transition-metal NHC complexes are of particular interest in carbene coordination chemistry,[27] the chemical shifts of the ^{13}C carbene resonances and the $^1J_{Rh-C}$ coupling constants for all complexes are provided in Table 2 and are consistent with previously reported spectra of similar Rh^{III} and Ir^{III} Cp* piano-stool complexes featuring N-heterocyclic carbene ligands.[28]

Table 2. ^{13}C NMR (101 MHz) Chemical Shifts and $^1J_{Rh-C}$ Coupling Constants of the Carbene Resonances for the Rh^{III} and Ir^{III} Cp^{*R} NHC Piano-Stool Complexes Featured in This Article

Rh complex	$\delta(^{13}C)$ (ppm)	$^1J_{Rh-C}$ (Hz)	Ir complex	$\delta(^{13}C)$ (ppm)
Rh-1	169.54	56.7	**Ir-1**	156.26
Rh-2	169.13	56.8	**Ir-2**	156.11
Rh-3	166.84	56.9		
Rh-4	167.04	57.4	**Ir-4**	153.53
Rh-5	184.47	55.8	**Ir-5**	170.50
			Ir-6	156.22
Rh-7	169.40	56.5	**Ir-7**	156.19
Rh-8	169.35	56.2		
Rh-9	169.46	56.3		
			Ir-10	156.35
Rh-11	168.11	56.4	**Ir-11**	154.41
Rh-12	183.11	55.5		
			Ir-13	155.74
Rh-14	169.03	56.5	**Ir-14**	155.89
Rh-15			**Ir-15**	152.09

X-ray Crystallography. Red or yellow single crystals suitable for X-ray diffraction ware obtained from vapor diffusion of hexanes or diethyl ether into saturated solutions of dichloromethane, acetone, or chloroform. Of the 12 new crystal structures solved, 10 crystals were found to belong to monoclinic space groups, with the remaining two crystals (**Rh-15** and **Ir-11**) belonging to orthorhombic space groups. The displacement ellipsoid plot of **Rh-4** is shown in Figure 5 as a

https://doi.org/10.1021/acs.organomet.1c00166
Organometallics 2021, 40, 1670−1681

representative example. Displacement ellipsoid plots for all crystal structures solved in this work are provided in the Supporting Information.

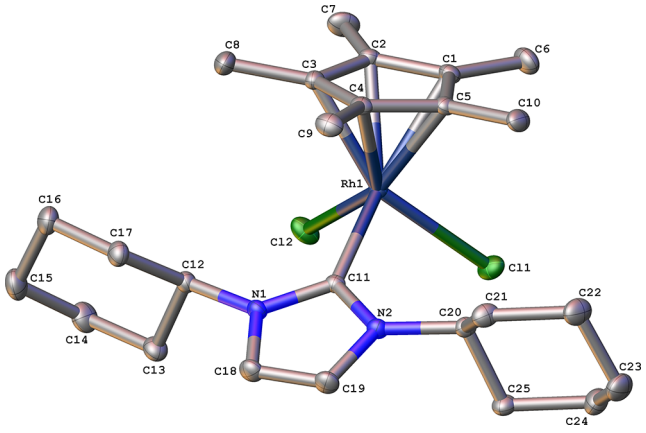

Figure 5. Displacement ellipsoid plot (50% probability) of **Rh-4**. Hydrogen atoms are omitted for clarity.

In all of the structures, the the M−Cp*C bond lengths *trans* to the NHC ligand are longer than than the *cis* or overlapping M−Cp*C bonds and increase in length upon the incorporation of more strongly σ-donating NHC ligands. Complexes featuring alkyl or aryl R substituents on the Cp*^{R} moiety were found to rotate such that the R group was oriented to some degree *anti* to the NHC ligand (Figure 6 and Table 3). These

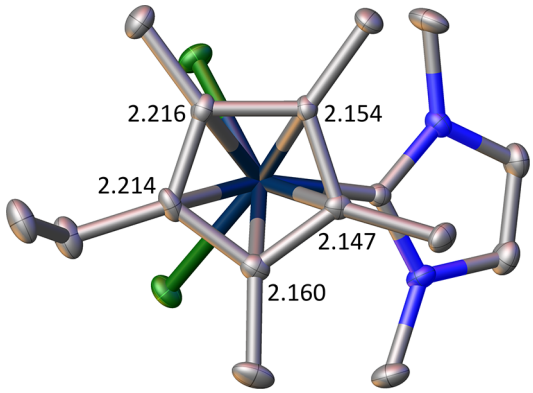

Figure 6. Displacement ellipsoid plot (50% probability) of **Ir-6** depicting the lengthened Cp*C bonds *anti* to the NHC ligand as a consequence of the *trans* influence (Å).

examples illustrate the *trans* influence brought about by strongly σ donating NHC ligands, a phenomenon that has previously been observed in the crystal structures of similar Rh^{III} and Ir^{III} Cp* NHC complexes.[29]

A search of the Cambridge Structural Database[30] (CSD) found 10 entries for similar Rh^{III} complexes and 44 entries for similar Ir^{III} Cp* complexes featuring monodentate NHC ligands. The Rh−C$_{carbene}$ bond lengths ranged from 2.047 to 2.070 Å, with a mean value of 2.057 Å, while the Ir−C$_{carbene}$ bond lengths ranged from 1.886 to 2.075 Å, with a mean value of 2.040 Å. The crystal structures solved in this work have Rh−C$_{carbene}$ bond lengths ranging from 2.043 to 2.068 Å, and Ir−C$_{carbene}$ bond lengths ranging from 2.044 to 2.050. All of these bond lengths fall within the range of those found in the CSD,

Table 3. Selected Average Bond Lengths for the (Cp*^{R})M(NHC)Cl$_2$ Crystal Structures Solved in This Work or Reported Previously

label	M−C$_{carbene}$ (Å)	M−Cp*C *cis*[a] (Å)	M−Cp* *trans*[a] (Å)
Rh-1[22]	2.050	2.150	2.223
Rh-3	2.068	2.154	2.225
Rh-4	2.0557	2.148	2.242
Rh-5[15]	2.049	2.153	2.217
Rh-8	2.056	2.158	2.212
Rh-14	2.053	2.146	2.212
Rh-15	2.043	2.158	2.233
Ir-1[23]	2.06	2.16	2.25
Ir-2	2.05	2.15	2.23
Ir-4	2.047	2.145	2.240
Ir-5[26]	2.038	2.14	2.25
Ir-6	2.050	2.156	2.212
Ir-7	2.050	2.158	2.220
Ir-11	2.047	2.168	2.196
Ir-13	2.048	2.155	2.221
Ir-14	2.044	2.152	2.221

[a]Defined as *cis* or *trans* relative to the NHC ligand.

with the exception of **Rh-15**, which features an electron-withdrawing Cp*^{C6F5} moiety.

For structures containing underivatized Cp* ligands, the Rh−C$_{carbene}$ bond lengths range from 2.049 to 2.068 Å while the Ir−C$_{carbene}$ bond lengths range from 2.038 to 2.06 Å. Upon comparison of the M−C$_{carbene}$ lengths in the underivatized Cp* complexes featuring different NHC ligands, it is apparent that stronger σ-donor NHC ligands do not necessarily lead to shorter M−C$_{carbene}$ bonds as might be expected. In some cases, this is attributable to steric effects arising from bulkier NHC N-substituents, as seen in the I^{i}Pr-containing **Rh-3** (2.068 Å) and the ICy-containing **Rh-4** (2.0557 Å). Non-negligible π-back-bonding interactions from the metal center to the carbene carbon also likely influence the M−C$_{carbene}$ bond distances, as the shortest M−C$_{carbene}$ bond lengths are observed for the previously reported **Rh-5** (2.049 Å) and **Ir-5** (2.038 Å) crystal structures featuring the Me$_2$-bimy NHC ligand, despite Me$_2$-bimy being the weakest σ-donor of all the NHC ligands in this study. This suggests benzimidazol-2-ylidene NHC scaffolds experience a larger degree of π-back-donation from the metal center in comparison to imidazol-2-ylidene scaffolds.[31]

In the derivatized Cp*^{R} complexes, the M−C$_{carbene}$ bond lengths are sensitive to the nature of the alkyl and aryl R substituents. Incorporation of an isopropyl group in **Rh-8** (2.068 Å) or phenethyl group in **Rh-14** (2.053 Å) slightly increases the Rh−C$_{carbene}$ bond lengths in comparison to that of **Rh-1** (2.050 Å). The opposite effect is observed for the crystal structure of **Rh-15**, with the electron-withdrawing pentafluorophenyl substituent giving rise to the shortest Rh−C$_{carbene}$ bond (2.043 Å) of all the rhodium structures. In contrast to the rhodium structures, the Ir−C$_{carbene}$ bond lengths featuring derivatized Cp*^{R} ligands are all shorter than those seen in the crystal structure of **Ir-1** (2.06 Å).

Antimicrobial Activity. Previous investigations in the Merola group have shown that Rh^{III} and Ir^{III} Cp*^{R} piano-stool complexes display promising antimicrobial activity, particularly against *M. smegmatis* (which frequently serves as a model to investigate more pathogenic mycobacteria), *S. aureus*, and MRSA. The activity was generally enhanced in complexes

https://doi.org/10.1021/acs.organomet.1c00166
Organometallics 2021, 40, 1670−1681

featuring hydrophobic substituents on the Cp^{*R} moiety and other coligands. Given these previous results in addition to the recent literature reports on the biological applications of organometallic complexes containing N-heterocyclic carbene ligands, we became interested in assessing the antimicrobial activity of these Rh^{III} and Ir^{III} Cp^{*R} NHC piano-stool complexes. Since the antimicrobial properties of these complexes have not been extensively studied up to this point, a wide scope of NHC and Cp^{R} ligands were employed.

Broad Panel Screening. The complexes were initially screened for antimicrobial activity against a broad microbial panel of various bacteria, yeast, and fungi. The activity was measured using the sequential dilution technique in 96-well plates, and the results were recorded as the minimum inhibitory concentration (MIC), which is the highest concentration at which no cell growth was detected in a well. A complete procedure for the antimicrobial studies conducted here is provided in the Experimental Section.

The majority of these complexes displayed moderate (defined here as ≤15 μM) to high (≤1 μM) activity against Gram-positive *Mycobacterium smegmatis* (Table 4). Rhodium complexes were generally found to have greater activities in comparison to those of iridium, both in a direct comparison of analogous complexes as well as within the data set taken as a whole. There are a few exceptions to this trend, with higher activity being observed for the iridium Cp* complex featuring Me_2-bimy (**Ir-5**) as well as the iridium $Cp^{*phenyl}$ complex featuring IMe (**Ir-11**).

Table 4. Antimicrobial Activities of Rh^{III} and Ir^{III} Cp^{*R} NHC Piano-Stool Complexes and NHC Ligand Precursors against *M. smegmatis*[a]

Rh complex or reference	MIC (μM)[b]	Ir complex	MIC (μM)[b]
Rh-1	4.9	**Ir-1**	8.1
Rh-2	0.58	**Ir-2**	31
Rh-3	1.1		
Rh-4	0.46	**Ir-4**	1.6
Rh-5	1.1	**Ir-5**	0.92
		Ir-6	16
Rh-7	0.58		
Rh-8	0.58		
Rh-9	0.54		
		Ir-10	1.7
Rh-11	1.1	**Ir-11**	0.45
Rh-12	0.97		
		Ir-13	3.5
Rh-14	2.0	**Ir-14**	6.8
		Ir-15	190
reference compounds			
ciprofloxacin	0.75		
streptomycin	0.43		

[a]Ciprofloxacin and streptomycin were also screened as positive controls. [b]Complexes were tested against *M. smegmatis* in duplicate. Both independent tests were found to give the same results.

Variation of the NHC ligand had a notable effect on activity, as seen when MICs of the underivatized Cp* complexes were compared. The activity is greatly enhanced for the rhodium complexes containing more hydrophobic NHC ligands (**Rh-2**, **Rh-3**, **Rh-4**, and **Rh-5**) in comparison to that of IMe (**Rh-1**). While the iridium Cp* complexes generally follow the same trend, the IEt variant (**Ir-2**) is a noteworthy exception, displaying significantly lower activity against *M. smegmatis* than **Ir-1**, **Ir-4**, and **Ir-5**. The activity is also highly sensitive to changes in the Cp^{*R} moieties. For rhodium complexes having the same NHC ligand (IMe) but different alkyl- or aryl-substituted Cp^{*R} rings, longer chain or branched alkyl R groups (**Rh-7**, **Rh-8**, and **Rh-9**) enhanced the activity in comparison to **Rh-1**. However, the iridium Cp^{*R} complexes featuring the IMe NHC ligand benefited more from incorporation of a phenyl-substituted Cp^{*R}, as **Ir-11** was found to be significantly more potent than **Ir-1** and gave the lowest MIC of all the complexes screened (0.45 μM). Despite these rhodium and iridium piano-stool analogues having a number of similarities with regard to structure and chemical reactivity, it is apparent that their structure−activity relationships and antimicrobial properties differ.

A few of the complexes also showed activity against other microbes in the broad panel (MIC data against all microbes tested in the broad panel are provided in Table S1 of the Supporting Information). The rhodium Cp* complex incorporating the ICy NHC ligand (**Rh-4**) gave moderate activity (15 μM) against Gram-positive MRSA and Gram-negative *E. coli*, while the iridium complex featuring an octyl substituent on the Cp^{*R} ring (**Ir-10**) displayed moderate to high activity against practically all microbes in the broad panel, most notably against MRSA (6.8 μM) and Gram-positive *S. aureus* (14 μM). Overall, the complexes were more effective against Gram-positive in comparison to Gram-negative strains in the broad panel, and in general, the activity increased with the hydrophobicity of the NHC and Cp^{*R} ligands.

In order to gain additional insight into the effect the NHC ligands have on the antimicrobial properties of these complexes, the imidazolium salt precursors were also screened against all microbes in the broad panel (Table S1), and their MICs against *M. smegmatis* are provided in Table 5. In all cases, the imidazolium salts were relatively inactive (>900 μM), suggesting that the antimicrobial activity in this system does not arise from solely from the NHC ligands.

Table 5. Antimicrobial Activities of NHC Ligand Precursors against *M. smegmatis*

NHC precursor	MIC (μM)
IMe·I	>1100
IEt·I	>990
Pr·Cl	>1300
I^{i}ICy·Cl	920
Me_2-bimy·I	>910

The silver complex precursors were not tested in this work, as they were generated *in situ* and subsequently reacted directly with the metal precursors. Attempts were made to isolate the silver-NHC complexes early in the project, but many of them were found to form complicated polymeric structures when they were removed from solution. This both greatly diminished their solubility and would not be representative of the relevant silver complex; thus, we did not pursue this further. On the basis of our analyses, we are confident that there is an insignificant amount of silver, if any, in our tested complexes.

To further investigate the influence of the NHC ligands on antimicrobial activity, the MICs of the $(Cp^{*R})M(NHC)Cl_2$ complexes against *M. smegmatis* were then compared on a 1:1 metal center basis to the MIC of the parental unit

https://doi.org/10.1021/acs.organomet.1c00166
Organometallics 2021, 40, 1670−1681

$[(Cp^{*R})MCl_2]_2$ from which they were derived, consisting of the same Cp^{*R} ligand and metal (Table 6). Incorporation of an

Table 6. Comparison of MICs (μM) against *M. smegmatis* between the $(Cp^{*R})M(NHC)Cl_2$ Complexes and Their Respective Parental Units

		complex		
Cp^{*R}	NHC	label	MIC	parent MIC
methyl	IMe	**Rh-1**	4.9	3.2
	IEt	**Rh-2**	0.58	
	I^{i}Pr	**Rh-3**	1.1	
	ICy	**Rh-4**	0.46	
	Me_2-bimy	**Rh-5**	1.1	
propyl	IMe	**Rh-7**	0.58	5.9
pentyl	IMe	**Rh-9**	0.54	2.7
phenyl	IMe	**Rh-11**	1.1	10
	Me_2-bimy	**Rh-12**	0.97	
phenethyl	IMe	**Rh-14**	2.0	40
methyl	IMe	**Ir-1**	8.1	10
	IEt	**Ir-2**	31	
	ICy	**Ir-4**	1.6	
	Me_2-bimy	**Ir-5**	0.92	
ethyl	IMe	**Ir-6**	16	19
octyl	IMe	**Ir-10**	1.7	16
phenyl	IMe	**Ir-11**	0.45	70
benzyl	IMe	**Ir-13**	3.5	8.4
phenethyl	IMe	**Ir-14**	6.8	33
C_6F_5	IMe	Ir-15	190	450

NHC ligand enhanced the activity in almost all cases, with the largest improvement observed for the $Cp^{*phenyl}$-containing **Ir-11**, giving over a 150-fold increase in activity upon inclusion of the IMe NHC ligand. These findings support the notion that the high antimicrobial activity displayed by these complexes does not solely arise from just the Cp^{*R} noble-metal parental units or individual NHC ligands via *in vivo* dissociation of the complexes. Instead, all the various structural features working in concert affect the overall activity of any particular complex, most likely by affecting the stability, bioavailability, and lipophilicity.

Mycobacterial Panel Screening. Due to the promising activities observed against *M. smegmatis* in the broad panel testing, a selection of these compounds was also screened against a panel of more pathogenic strains of mycobacteria. Antimicrobial activities are reported in Table S2 in the Supporting Information as MICs (μg/mL and μM) for all compounds as well as for streptomycin.

As seen in the broad panel testing, the rhodium complexes were generally more active than the iridium variants. Both **Rh-3** and **Rh-9** displayed moderate activity against *M. intracellulare* (8.7 μM), while a range of the complexes also gave moderate activity against *M. chimaera*, the most potent being **Rh-4** (7.4 μM). Other notable results include **Rh-3** against *M. avium* (17 μM), as well as **Rh-8** against *M. abscessus* (19 μM). Despite being the most potent against *M. smegmatis* of all the complexes screened in the broad panel, **Ir-11** showed relatively poor activity against the mycobacterial panel, with the exceptions of *M. intracellulare* and *M. chimaera* (14 μM).

Stability Studies. In order to assess the stability of the piano-stool complexes, ^{1}H NMR spectra of **Rh-4** and **Ir-1** were acquired over a period of 72 h in D_2O with 0.1% DMSO to mimic the antimicrobial testing conditions (Figures S1 and S2). Both complexes proved to be stable in this media after 3 days, with the NMR spectra showing minimal change and no indication of ligand dissociation over the monitored time period. Furthermore, HRMS analysis of the complexes revealed that the NHC and Cp^{*R} ligands are still coordinated to the metal center, with the $[(Cp^{*R})M(NHC)Cl]^+$ fragments being observed for all complexes (representative HRMS traces are shown in Figures S3 and S4).

Cytotoxicity Studies. To investigate if noble-metal NHC piano-stool complexes of this type are detrimental to mammalian cells, complex **Rh-4** was screened for toxicity against Vero E6 cell lines (kidney epithelial cells extracted from an African green monkey) and Calu-3 cell lines (representative of human lung epithelial cells) (Figure 7). In general, **Rh-4** was

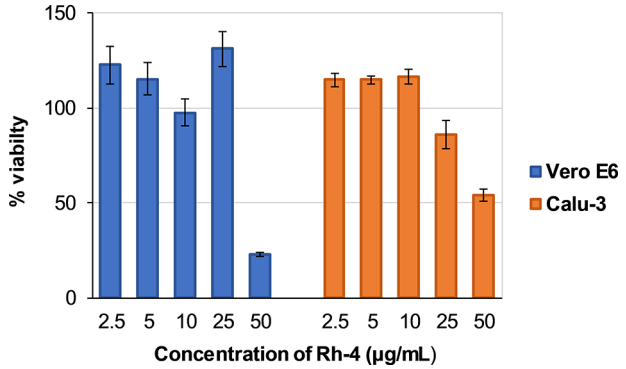

Figure 7. Cytotoxicity of **Rh-4** against Vero E6 and Calu-3 cell lines, where a high percent viability at any given concentration indicates low toxicity.

found to be nontoxic toward these mammalian cells, except at elevated concentrations of 50 μg/mL (92 μM). Considering that **Rh-4** was active against *M. smegmatis* at concentrations as low as 0.25 μg/mL (0.46 μM), these results are highly encouraging.

CONCLUSION

The work described in this article expands upon continuing investigations into the biological properties of noble-metal piano-stool complexes featuring N-heterocyclic carbene ligands. A modest library of $(Cp^{*R})M(NHC)Cl_2$ (M = Rh, Ir) complexes was synthesized, characterized, and screened for antimicrobial activity against a range of microbes, with many of the complexes displaying excellent activity (>1 μM) against *Mycobacterium smegmatis*. The rhodium complexes were generally found to be more active than iridium complexes, and the activity was enhanced upon inclusion of more hydrophobic Cp^{*R} and NHC ligands, which is in agreement with previous studies by the Merola group[18−20] and others.[15] Cytotoxicity tests on **Rh-4** showed that this compound is only toxic toward mammalian Vero E6 and Calu-3 cell lines at concentrations 200-fold higher (92 μM) than the observed activity against *M. smegmatis* (0.46 μM). Overall, these findings highlight the promising utility of N-heterocyclic carbene and Cp^{*R} moieties for the development and tunability of noble-metal piano-stool antimicrobial agents.

EXPERIMENTAL SECTION

Materials. Reagent-grade solvents and all materials for synthesis, purification, and characterization were purchased from commercial

https://doi.org/10.1021/acs.organomet.1c00166
Organometallics 2021, 40, 1670−1681

sources and used as received unless otherwise stated. The NHC ligand precursors 1,3-dimethylimidazolium iodide (IMe·I),[32] 1,3-diethylimidazolium iodide (IEt·I),[33] and 1,3-dimethylbenzimidazolium iodide (Me_2-bimy·I)[34] were synthesized as reported previously. Both 1,3-diisopropylimidazolium chloride (I^iPr·Cl) and 1,3-dicyclohexylimidazolium chloride (ICy·Cl), as well as silver(I) oxide, were purchased from Sigma-Aldrich (St. Louis, MO). Rhodium and iridium dimers of the form $[(Cp^{*R})MCl_2]_2$ (R = alkyl or aryl)[35] were synthesized as reported previously using rhodium(III) chloride hydrate and iridium(III) chloride hydrate precursors purchased from Pressure Chemical (Pittsburgh, PA). Deuterated solvents for NMR spectroscopy were obtained from Cambridge Isotope Laboratories (Tewksbury, MA).

Instrumentation. ^{1}H, ^{13}C, and ^{19}F NMR spectra were collected on an Agilent U4-DD2 or Agilent MR4 400 MHz spectrometer. ^{13}C NMR spectra were correspondingly recorded at 101 MHz and ^{19}F NMR at 376 MHz. Elemental analyses were performed by Atlantic Microlabs (Norcross, GA). High-resolution mass spectra were collected on an Agilent 6220 Accurate Mass TOF LC-MS instrument. X-ray crystallographic data were collected at 100 K on a Rigaku Oxford Diffraction Gemini E Ultra diffractometer or a Rigaku Oxford Diffraction Synergy operating with either Mo Kα or Cu Kα radiation. Crystals were coated in Paratone oil and mounted on a fiber. Data collection and data reduction were performed using Agilent's CrysAlisPro software.[36] Structure solution was performed using SHELXT[37] and refined using SHELXL[38] via Olex2. The final refinement model involved anisotropic displacement parameters for non-hydrogen atoms and a riding model for all hydrogen atoms. Olex2 was used for molecular graphics generation.[39] Searches of the Cambridge Structural Database (CSD)[30] were carried out using the program Conquest,[40] and the results were analyzed with the statistical functions of the program Mercury.[41]

Synthesis and Characterization: General Synthesis of $(Cp^{*R})M(NHC)Cl_2$ Complexes. A Schlenk flask was charged with the appropriate amount of the desired imidazolium salt and silver(I) oxide in dichloromethane (15 mL) under an atmosphere of nitrogen. The mixture was stirred magnetically in the dark for 4 h. The desired rhodium or iridium $[(Cp^{*R})MCl_2]_2$ dimer was then added, and the mixture was stirred for an additional 12 h, over which time the color changed from gray to dark red (Rh) or dark yellow (Ir). After the elapsed time, the suspension was filtered through Celite and the solvent removed by rotary evaporation. The products were purified via recrystallization from dichloromethane and hexanes and isolated on a frit as red (Rh) or yellow (Ir) solids.

Synthesis of ***Rh-1***. Following the general procedure, 1,3-dimethylimidazolium iodide (0.2284 g, 1.0193 mmol), silver(I) oxide (0.1653 g, 0.7135 mmol), and $[(Cp^*)RhCl_2]_2$ (0.3000 g, 0.4854 mmol) were reacted in dichloromethane to give **Rh-1** (0.3517 g, 89%). Characterization data were consistent with previously reported data.[22]

Synthesis of ***Rh-2***. Following the general procedure, 1,3-diethylimidazolium iodide (0.0857 g, 0.3398 mmol), silver(I) oxide (0.0501 g, 0.2378 mmol), and $[(Cp^*)RhCl_2]_2$ (0.1000 g, 0.1618 mmol) were reacted in dichloromethane to give **Rh-2** (0.1124 g, 80%). ^{1}H NMR (400 MHz, $CDCl_3$, δ): 7.09 (s, 2H, $CH_{backbone}$), 4.87−4.70 (m, 2H, NCH_2CH_3), 4.04−3.97 (m, 2H, NCH_2CH_3), 1.57 (s, 15H, Cp^*CH_3), 1.45 (t, J = 7.2 Hz, 6H, NCH_2CH_3). ^{13}C NMR (101 MHz, $CDCl_3$, δ): 169.1 (d, J = 56.8 Hz, $C_{carbene}$), 122.0 (d, J = 0.8 Hz, $CH_{backbone}$), 96.2 (d, J = 7.0 Hz, Cp^*C), 45.9 (NCH_2CH_3) 16.9 (NCH_2CH_3), 9.4 (Cp^*CH_3). HRMS/ESI+ (m/z): calcd for $C_{17}H_{27}ClN_2Rh$, 397.0912; found, 397.0909. Anal. Calcd for $C_{17}H_{27}Cl_2N_2Rh{\cdot}0.5H_2O$: C, 46.17; H, 6.38. Found: C, 46.09; H, 6.12.

Synthesis of ***Rh-3***. Following the general procedure, 1,3-diisopropylimidazolium chloride (0.0641 g, 0.3398 mmol), silver(I) oxide (0.0551 g, 0.2378 mmol), and $[(Cp^*)RhCl_2]_2$ (0.1000 g, 0.1618 mmol) were reacted in dichloromethane to give **Rh-3** (0.0852 g, 57%). ^{1}H NMR (400 MHz, $CDCl_3$, δ): 7.08 (s, 2H, $CH_{backbone}$), 5.32 (hept, J = 6.5 Hz, 2H, $NCH(CH_3)_2$), 1.62 (s, 15H, Cp^*CH_3), 1.51 (d, J = 6.3 Hz, 6H, $NCH(CH_3)_2$), 1.41 (d, J = 6.8 Hz, 6H, $NCH(CH_3)_2$). ^{13}C NMR (101 MHz, $CDCl_3$, δ): 166.8 (d, J = 56.9 Hz, $C_{carbene}$), 119.5 (d, J = 0.9 Hz, $CH_{backbone}$), 96.3 (d, J = 7.0 Hz, Cp^*C), 51.8 ($NCH(CH_3)_2$)), 25.4 ($NCH(CH_3)_2$), 25.2 ($NCH(CH_3)_2$), 9.5 (Cp^*CH_3). HRMS/ESI+ (m/z): calcd for $C_{19}H_{31}ClN_2Rh$, 425.1231; found, 425.1238.

Synthesis of ***Rh-4***. Following the general procedure, 1,3-dicyclohexylimidazolium chloride (0.0913 g, 0.3398 mmol), silver(I) oxide (0.0551 g, 0.2378 mmol), and $[(Cp^*)RhCl_2]_2$ (0.1000 g, 0.1618 mmol) were reacted in dichloromethane to give **Rh-4** (0.1752 g, 75%). ^{1}H NMR (400 MHz, $CDCl_3$, δ): 7.06 (s, 2H, $CH_{backbone}$), 4.87 (tt, J = 11.8, 3.5 Hz, 2H, $NCH_{cyclohexyl}$), 2.52 (d, J = 11.9 Hz, 2H, $CH_{2cyclohexyl}$), 1.96−1.65 (m, 12H, $CH_{2cyclohexyl}$), 1.62 (s, 15H, Cp^*CH_3), 1.59−1.10 (m, 6H, $CH_{2cyclohexyl}$). ^{13}C NMR (101 MHz, $CDCl_3$, δ): 167.0 (d, J = 57.4 Hz, $C_{carbene}$), 119.8 (d, J = 1.0 Hz, $CH_{backbone}$) 96.2 (d, J = 7.0 Hz, Cp^*C), 58.8 ($NCH_{cyclohexyl}$), 35.8 ($CH_{2cyclohexyl}$), 35.6 ($CH_{2cyclohexyl}$), 25.9 ($CH_{2cyclohexyl}$), 25.5 ($CH_{2cyclohexyl}$), 25.4 ($CH_{2cyclohexyl}$), 9.6 (Cp^*CH_3). HRMS/ESI+ (m/z): calcd for $C_{25}H_{39}ClN_2Rh$, 505.1851; found, 505.1850. Anal. Calcd for $C_{25}H_{39}Cl_2N_2Rh$: C, 55.46; H, 7.26. Found: C, 55.01; H, 7.43.

Synthesis of ***Rh-5***. Following the general procedure, 1,3-dimethylbenzimidazolium iodide (0.0931 g, 0.3398 mmol), silver(I) oxide (0.0551 g, 0.2378 mmol), and $[(Cp^*)RhCl_2]_2$ (0.1000 g, 0.1618 mmol) were reacted in dichloromethane to give **Rh-5** (0.1281 g, 87%). Characterization data were consistent with previously reported data.[15a]

Synthesis of ***Rh-7***. Following the general procedure, 1,3-dimethylimidazolium iodide (0.0698 g, 0.3115 mmol), silver(I) oxide (0.0505 g, 0.2180 mmol), and $[(Cp^{*propyl})RhCl_2]_2$ (0.1000 g, 0.1483 mmol) were reacted in dichloromethane to give **Rh-7** (0.0776 g, 60%). ^{1}H NMR (400 MHz, $CDCl_3$, δ): 6.98 (s, 2H, $CH_{backbone}$), 4.00 (s, 6H, NCH_3), 2.05−1.97 (m, 2H, $Cp^*CH_2CH_2CH_3$), 1.66 (s, 6H, Cp^*CH_3), 1.60 (s, 6H, Cp^*CH_3), 1.45−1.37 (m, 2H, $Cp^*CH_2CH_2CH_3$), 0.92 (t, J = 7.4 Hz, 3H, $Cp^*CH_2CH_2CH_3$). ^{13}C NMR (101 MHz, $CDCl_3$, δ): 169.4 (d, J = 56.5 Hz, $C_{carbene}$), 124.3 (d, J = 1.0 Hz, $CH_{backbone}$), 98.1 (d, J = 6.5 Hz, Cp^*C), 97.1 (d, J = 7.7 Hz, Cp^*C), 95.3 (d, J = 7.2 Hz, Cp^*C), 39.2, (NCH_3) 26.6 ($Cp^*CH_2CH_2CH_3$), 21.8 ($Cp^*CH_2CH_2CH_3$), 14.3 ($Cp^*CH_2CH_2CH_3$), 9.7 (Cp^*CH_3), 9.5 (Cp^*CH_3). HRMS/ESI+ (m/z): calcd for$C_{17}H_{27}ClN_2Rh$, 397.0912; found, 397.0908. Anal. Calcd for $C_{17}H_{27}Cl_2N_2Rh{\cdot}0.5H_2O$: C, 46.17; H, 6.38. Found: C, 46.03; H, 6.19.

Synthesis of ***Rh-8***. Following the general procedure, 1,3-dimethylimidazolium iodide (0.0698 g, 0.3115 mmol), silver(I) oxide (0.0505 g, 0.2180 mmol), and $[(Cp^{*isopropyl})RhCl_2]_2$ (0.1000 g, 0.1483 mmol) were reacted in dichloromethane to give **Rh-8** (0.0758 g, 59%). ^{1}H NMR (400 MHz, $CDCl_3$, δ): 6.98 (s, 2H, $CH_{backbone}$), 3.99 (s, 6H, NCH_3), 2.57 (hept, J = 7.0 Hz, 1H, $Cp^*CH(CH_3)_2$)), 1.67 (s, 6H, Cp^*CH_3), 1.59 (s, 6H, Cp^*CH_3), 1.19 (d, J = 7.1 Hz, 6H, $Cp^*CH(CH_3)_2$). ^{13}C NMR (101 MHz, $CDCl_3$, δ): 169.4 (d, J = 56.2 Hz, $C_{carbene}$), 124.2 (d, J = 1.0 Hz, $CH_{backbone}$), 103.1 (d, J = 7.0 Hz, Cp^*C), 96.9 (d, J = 6.9 Hz, Cp^*C), 95.8 (d, J = 7.3 Hz, Cp^*C), 39.3 (NCH_3), 26.2 ($Cp^*CH(CH_3)_2$)), 21.2 ($Cp^*CH(CH_3)_2$), 10.4 (Cp^*CH_3), 9.6 (Cp^*CH_3). HRMS/ESI+ (m/z): calcd for$C_{17}H_{27}ClN_2Rh$, 397.0912; found, 397.0888.

Synthesis of ***Rh-9***. Following the general procedure, 1,3-dimethylimidazolium iodide (0.0644 g, 0.2876 mmol), silver(I) oxide (0.0466 g, 0.2013 mmol), and $[(Cp^{*pentyl})RhCl_2]_2$ (0.1000 g, 0.1369 mmol) were reacted in dichloromethane to give **Rh-9** (0.0569 g, 45%). ^{1}H NMR (400 MHz, $CDCl_3$, δ): 6.99 (s, 2H, $CH_{backbone}$), 3.99 (s, 6H, NCH_3), 2.07−1.97 (m, 2H, $Cp^*CH_2(CH_2)_3CH_3$), 1.65 (s, 6H, Cp^*CH_3), 1.60 (s, 6H, Cp^*CH_3), 1.42−1.33 (m, 2H, $Cp^*CH_2(CH_2)_3CH_3$) 1.32−1.22 (m, 4H, $Cp^*CH_2(CH_2)_3CH_3$), 0.93−0.80 (m, 3H, $Cp^*CH_2(CH_2)_3CH_3$). ^{13}C NMR (101 MHz, $CDCl_3$, δ): 169.5 (d, J = 56.3 Hz, $C_{carbene}$), 124.3 (d, J = 1.0 Hz, $CH_{backbone}$), 98.0 (d, J = 6.6 Hz, Cp^*C), 97.5 (d, J = 7.5 Hz, Cp^*C), 95.3 (d, J = 7.2 Hz, Cp^*C), 39.2 (NCH_3), 32.0 ($Cp^*CH_2(CH_2)_3CH_3$), 28.3 ($Cp^*CH_2(CH_2)_3CH_3$), 24.7 ($Cp^*CH_2(CH_2)_3CH_3$), 22.5 ($Cp^*CH_2(CH_2)_3CH_3$), 14.0 ($Cp^*CH_2(CH_2)_3CH_3$), 9.6 (Cp^*CH_3), 9.5 (Cp^*CH_3). HRMS/ESI + (m/z): calcd for $C_{19}H_{31}ClN_2Rh$, 425.1231; found, 425.1239.

https://doi.org/10.1021/acs.organomet.1c00166
Organometallics 2021, 40, 1670−1681

Synthesis of ***Rh-11***. Following the general procedure, 1,3-dimethylimidazolium iodide (0.0254 g, 0.1132 mmol), silver(I) oxide (0.0184 g, 0.0792 mmol), and $[(Cp^{*phenyl})RhCl_2]_2$ (0.0040 g, 0.0539 mmol) were reacted in dichloromethane to give **Rh-11** (0.0395 g, 78%). ^{1}H NMR (400 MHz, $CDCl_3$, δ): 7.62−7.55 (m, 2H, Cp*Ph), 7.39−7.30 (m, 3H, Cp*Ph), 6.92 (s, 2H, $CH_{backbone}$), 3.83 (s, 6H, NCH_3), 1.75 (s, 6H, Cp*CH_3), 1.67 (s, 6H, Cp*CH_3). ^{13}C NMR (101 MHz, $CDCl_3$, δ): 168.1 (d, J = 56.4 Hz, $C_{carbene}$), 130.8 (Cp*Ph), 130.6 (Cp*Ph), 128.5 (Cp*Ph), 128.5 (Cp*Ph), 124.4 (d, J = 0.8 Hz, $CH_{backbone}$), 99.8 (d, J = 6.4 Hz, Cp*C), 96.9 (d, J = 6.7 Hz, Cp*C), 93.4 (d, J = 8.1 Hz, Cp*C), 39.2 (NCH_3), 10.9 (Cp*CH_3), 9.7 (Cp*CH_3). HRMS/ESI+ (m/z): calcd for $C_{20}H_{25}ClN_2Rh$, 431.0756; found, 431.0744.

Synthesis of ***Rh-12***. Following the general procedure, 1,3-dimethylbenzimidazolium iodide (0.0310 g, 0.1132 mmol), silver(I) oxide (0.0184 g, 0.0792 mmol), and $[(Cp^{*phenyl})RhCl_2]_2$ (0.0040 g, 0.0539 mmol) were reacted in dichloromethane to give **Rh-12** (0.0265 g, 48%). ^{1}H NMR (400 MHz, $CDCl_3$, δ): 7.67−7.63 (m, 2H, Cp*Ph), 7.38−7.28 (m, 7H, overlapped Cp*Ph, $CH_{backbone}$), 4.07 (s, 6H, NCH_3), 1.78 (s, 6H, Cp*CH_3), 1.73 (s, 6H, Cp*CH_3). ^{13}C NMR (101 MHz, $CDCl_3$, δ): 183.1 (d, J = 55.5 Hz, $C_{carbene}$), 136.0 (d, J = 1.0 Hz, $C_{bridgeheads}$), 130.62 (Cp*Ph), 130.57 (Cp*Ph), 128.60 (Cp*Ph), 128.55 (Cp*Ph), 123.5 ($CH_{backbone}$), 110.2 ($CH_{backbone}$), 101.2 (d, J = 6.4 Hz, Cp*C), 96.8 (d, J = 6.8 Hz, Cp*C), 94.3 (d, J = 7.6 Hz, Cp*C), 36.0 (NCH_3), 11.0 (Cp*CH_3), 9.9 (Cp*CH_3). HRMS/ESI+ (m/z): calcd for $C_{24}H_{27}ClN_2Rh$, 481.0912; found, 481.0910

Synthesis of ***Rh-14***. Following the general procedure, 1,3-dimethylimidazolium iodide (0.0589 g, 0.2631 mmol), silver(I) oxide (0.0427 g, 0.1841 mmol), and $[(Cp^{*phenethyl})RhCl_2]_2$ (0.1000 g, 0.1253 mmol) were reacted in dichloromethane to give **Rh-14** (0.0910 g, 73%). ^{1}H NMR (400 MHz, $CDCl_3$, δ): 7.26−7.16 (m, 3H, Cp*CH_2CH_2Ph), 7.03−6.98 (m, 2H, Cp*CH_2CH_2Ph), 6.94 (s, 2H, $CH_{backbone}$), 3.94 (s, 6H, NCH_3), 2.69 (t, J = 7.4 Hz, 2H, Cp*CH_2CH_2Ph), 2.33 (t, J = 7.4 Hz, 2H, Cp*CH_2CH_2Ph), 1.61 (s, 6H, Cp*CH_3), 1.36 (s, 6H, Cp*CH_3). ^{13}C NMR (101 MHz, $CDCl_3$, δ): 169.0 (d, J = 56.5 Hz, $C_{carbene}$), 140.2 (Cp*CH_2CH_2Ph), 128.7 (Cp*CH_2CH_2Ph), 128.64 (Cp*CH_2CH_2Ph), 126.61 (Cp*CH_2CH_2Ph), 124.3 (d, J = 1.0 Hz, $CH_{backbone}$), 98.0 (d, J = 6.5 Hz, Cp*C), 96.1 (d, J = 7.1 Hz, Cp*C), 95.4 (d, J = 7.6 Hz, Cp*C), 39.2 (NCH_3), 34.4 (Cp*CH_2CH_2Ph), 27.1 (Cp*CH_2CH_2Ph), 9.4 (Cp*CH_3), 9.3 (Cp*CH_3). HRMS/ESI+ (m/z): calcd for $C_{22}H_{29}ClN_2Rh$, 459.1074; found, 459.1077. Anal. Calcd for $C_{22}H_{29}Cl_2N_2Rh$: C, 53.35; H, 5.90. Found: C, 52.55; H, 6.09.

Synthesis of ***Rh-15***. Following the general procedure, 1,3-dimethylimidazolium iodide (0.0153 g, 0.0683 mmol), silver(I) oxide (0.0111 g, 0.0478 mmol), and $[(Cp^{*C_6F_5})RhCl_2]_2$ (0.0300 g, 0.0325 mmol) were reacted in dichloromethane to give **Rh-15** (0.0112 g, 31%). Well-resolved NMR spectra of **Rh-15** were not acquired, as a suitable amount of the sample was not isolated. However, the sample was characterized via HRMS and single-crystal X-ray diffraction. HRMS/ESI+ (m/z): calcd for $C_{20}H_{20}ClF_5N_2Rh$, 521.0290; found, 521.0301.

Synthesis of ***Ir-1***. Following the general procedure, 1,3-dimethylimidazolium iodide (0.1772 g, 0.7908 mmol), silver(I) oxide (0.1283 g, 0.5535 mmol), and $[(Cp^*)IrCl_2]_2$ (0.3000 g, 0.3765 mmol) were reacted in dichloromethane to give **Ir-1** (0.2792 g, 75%). Characterization data were consistent with previously reported data.[23]

Synthesis of ***Ir-2***. Following the general procedure, 1,3-diethylimidazolium iodide (0.0664 g, 0.2636 mmol), silver(I) oxide (0.0428 g, 0.1845 mmol), and $[(Cp^*)IrCl_2]_2$ (0.1000 g, 0.1255 mmol) were reacted in dichloromethane to give **Ir-2** (0.0887 g, 68%). Characterization data were consistent with previously reported data.[24]

Synthesis of ***Ir-4***. Following the general procedure, 1,3-dicyclohexylimidazolium chloride (0.0709 g, 0.2636 mmol), silver(I) oxide (0.0428 g, 0.1845 mmol), and $[(Cp^*)IrCl_2]_2$ (0.1000 g, 0.1255 mmol) were reacted in dichloromethane to give **Ir-4** (0.0781 g, 49%). Characterization data were consistent with previously reported data.[25]

Synthesis of ***Ir-5***. Following the general procedure, 1,3-dimethylbenzimidazolium iodide (0.0723 g, 0.2636 mmol), silver(I) oxide (0.0428 g, 0.1845 mmol), and $[(Cp^*)IrCl_2]_2$ (0.1000 g, 0.1255 mmol) were reacted in dichloromethane to give **Ir-5** (0.1119 g, 82%). Characterization data were consistent with previously reported data.[26]

Synthesis of ***Ir-6***. Following the general procedure, 1,3-dimethylimidazolium iodide (0.0570 g, 0.2546 mmol), silver(I) oxide (0.0413 g, 0.1782 mmol), and $[(Cp^{*ethyl})IrCl_2]_2$ (0.1000 g, 0.1212 mmol) were reacted in dichloromethane to give **Ir-6** (0.0847 g, 69%). ^{1}H NMR (400 MHz, $CDCl_3$, δ): 6.90 (s, 2H, $CH_{backbone}$), 3.95 (s, 6H, NCH_3), 1.99 (q, J = 7.6 Hz, 2H, Cp*CH_2CH_3), 1.67 (s, 6H, Cp*CH_3), 1.63 (s, 6H, Cp*CH_3), 1.07 (t, J = 7.6 Hz, 3H, Cp*CH_2CH_3). ^{13}C NMR (101 MHz, $CDCl_3$, δ): 156.2 ($C_{carbene}$), 123.3 ($CH_{backbone}$), 90.8 (Cp*C), 89.9 (Cp*C), 87.8 (Cp*C), 38.7 (NCH_3), 18.0 (Cp*CH_2CH_3), 12.9 (Cp*CH_2CH_3), 9.12 (Cp*CH_3), 9.08 (Cp*CH_3). HRMS/ESI+ (m/z): calcd for $C_{16}H_{25}Cl[^{193}Ir]N_2$, 473.1335; found, 473.1284.

Synthesis of ***Ir-7***. Following the general procedure, 1,3-dimethylimidazolium iodide (0.0552 g, 0.2462 mmol), silver(I) oxide (0.0399 g, 0.1724 mmol), and $[(Cp^{*propyl})IrCl_2]_2$ (0.1000 g, 0.1173 mmol) were reacted in dichloromethane to give **Ir-7** (0.0342 g, 28%). ^{1}H NMR (400 MHz, $CDCl_3$, δ): 6.91 (s, 2H, $CH_{backbone}$), 3.94 (s, 6H, NCH_3), 1.99−1.92 (m, 2H, Cp*$CH_2CH_2CH_3$), 1.65 (s, 6H, Cp*CH_3), 1.62 (s, 6H, Cp*CH_3), 1.45 (sextet, J = 7.6 Hz, 2H, Cp*$CH_2CH_2CH_3$), 0.92 (t, J = 7.4 Hz, 3H, Cp*$CH_2CH_2CH_3$). ^{13}C NMR (101 MHz, $CDCl_3$, δ): 156.2 ($C_{carbene}$), 123.3 ($CH_{backbone}$), 90.5 (Cp*C), 89.1 (Cp*C), 88.1 (Cp*C), 38.7 (NCH_3), 26.6 (Cp*$CH_2CH_2CH_3$), 21.9 (Cp*$CH_2CH_2CH_3$), 14.4 (Cp*$CH_2CH_2CH_3$), 9.4 (Cp*CH_3), 9.1 (Cp*CH_3). HRMS/ESI+ (m/z): calcd for $C_{17}H_{27}Cl[^{193}Ir]N_2$, 487.1487; found, 487.1480.

Synthesis of ***Ir-10***. Following the general procedure, 1,3-dimethylimidazolium iodide (0.0474 g, 0.2115 mmol), silver(I) oxide (0.0343 g, 0.1480 mmol), and $[(Cp^{*octyl})IrCl_2]_2$ (0.1000 g, 0.1007 mmol) were reacted in dichloromethane to give **Ir-10** (0.0602 g, 50%). 6.91 (s, 2H, $CH_{backbone}$), 3.96 (s, 6H, NCH_3), 2.01−1.93 (m, 2H, Cp*$CH_2(CH_2)_6CH_3$), 1.66 (s, 6H, Cp*CH_3), 1.63 (s, 6H, Cp*CH_3), 1.45−1.20 (m, 12H, Cp*$CH_2(CH_2)_6CH_3$), 0.94−0.81 (m, 3H, Cp*$CH_2(CH_2)_6CH_3$). ^{13}C NMR (101 MHz, $CDCl_3$, δ): 156.4 ($C_{carbene}$), 123.3 ($CH_{backbone}$), 90.4 (Cp*C), 89.5 (Cp*C), 88.1 (Cp*C), 38.8 (NCH_3), 31.9 (Cp*$CH_2(CH_2)_6CH_3$), 30.0 (Cp*$CH_2(CH_2)_6CH_3$), 29.5 (Cp*$CH_2(CH_2)_6CH_3$), 29.3 (Cp*$CH_2(CH_2)_6CH_3$), 28.8 (Cp*$CH_2(CH_2)_6CH_3$), 24.7 (Cp*$CH_2(CH_2)_6CH_3$), 22.8 (Cp*$CH_2(CH_2)_6CH_3$), 14.2 (Cp*$CH_2(CH_2)_6CH_3$), 9.4 (Cp*CH_3), 9.2 (Cp*CH_3). HRMS/ESI+ (m/z): calcd for $C_{22}H_{37}Cl[^{193}Ir]N_2$, 557.2275; found, 557.2293.

Synthesis of ***Ir-11***. Following the general procedure, 1,3-dimethylimidazolium iodide (0.0512 g, 0.2283 mmol), silver(I) oxide (0.0370 g, 0.1598 mmol), and $[(Cp^{*phenyl})IrCl_2]_2$ (0.1000 g, 0.1087 mmol) were reacted in dichloromethane to give **Ir-11** (0.0970 g, 80%). ^{1}H NMR (400 MHz, $CDCl_3$, δ): 7.56−7.50 (m, 2H, Cp*Ph), 7.37−7.29 (m, 3H, Cp*Ph), 6.85 (s, 2H, $CH_{backbone}$), 3.81 (s, 6H, NCH_3), 1.74 (s, 6H, Cp*CH_3), 1.68 (s, 6H, Cp*CH_3). ^{13}C NMR (101 MHz, $CDCl_3$, δ): 154.4 ($C_{carbene}$), 131.8 (Cp*Ph), 130.3 (Cp*Ph), 128.4 (Cp*Ph), 127.9 (Cp*Ph), 123.3 ($CH_{backbone}$), 93.3 (Cp*C), 88.8 (Cp*C), 85.0 (Cp*C), 38.6 (NCH_3), 10.3 (Cp*CH_3), 9.3 (Cp*CH_3). HRMS/ESI+ (m/z): calcd for $C_{20}H_{25}Cl[^{193}Ir]N_2$, 521.1330; found, 521.1291. Anal. Calcd for $C_{20}H_{25}Cl_2IrN_2{\cdot}0.5H_2O$: C, 42.47; H, 4.63. Found: C, 42.29; H, 4.58.

Synthesis of ***Ir-13***. Following the general procedure, 1,3-dimethylimidazolium iodide (0.0496 g, 0.2213 mmol), silver(I) oxide (0.0359 g, 0.1549 mmol), and $[(Cp^{*benzyl})IrCl_2]_2$ (0.1000 g, 0.1054 mmol) were reacted in dichloromethane to give **Ir-13** (0.0851 g, 71%). ^{1}H NMR (400 MHz, $CDCl_3$, δ): 7.31−7.27 (m, 2H, Cp*CH_2Ph), 7.25−7.18 (m, 1H, Cp*CH_2Ph), 7.13−7.09 (m, 2H, Cp*CH_2Ph), 6.94 (s, 2H, $CH_{backbone}$), 4.00 (s, 6H, NCH_3), 3.44 (s, 2H, Cp*CH_2Ph), 1.66 (s, 6H, Cp*CH_3), 1.65 (s, 6H, Cp*CH_3). ^{13}C NMR (101 MHz, $CDCl_3$, δ): 155.7 ($C_{carbene}$), 137.8 (Cp*Ph), 128.8 (Cp*Ph), 128.3 (Cp*Ph), 126.8 (Cp*Ph), 123.4 ($CH_{backbone}$), 90.2 (Cp*C), 88.82 (Cp*C), 88.78 (Cp*C), 38.8 (NCH_3), 30.5

https://doi.org/10.1021/acs.organomet.1c00166
Organometallics 2021, 40, 1670−1681

(Cp^*CH_2Ph), 9.7 (Cp^*CH_3), 9.4 (Cp^*CH_3). HRMS/ESI+ (m/z): calcd for $C_{21}H_{27}Cl[^{193}Ir]N_2$, 535.1487; found, 535.1437.

Synthesis of ***Ir-14***. Following the general procedure, 1,3-dimethylimidazolium iodide (0.0482 g, 0.2150 mmol), silver(I) oxide (0.0349 g, 0.1505 mmol), and $[(Cp^{*phenethyl})IrCl_2]_2$ (0.1000 g, 0.1024 mmol) were reacted in dichloromethane to give **Ir-14** (0.0797 g, 67%). ^{1}H NMR (400 MHz, $CDCl_3$, δ): 7.27−7.15 (m, 3H, $Cp^*CH_2CH_2Ph$), 7.08−7.00 (m, 2H, $Cp^*CH_2CH_2Ph$), 6.87 (s, 2H, $CH_{backbone}$), 3.91 (s, 6H, NCH_3), 2.72 (t, J = 7.4 Hz, 2H, $Cp^*CH_2CH_2Ph$), 2.27 (t, J = 7.4 Hz, 2H, $Cp^*CH_2CH_2Ph$), 1.64 (s, 6H, Cp^*CH_3), 1.41 (s, 6H, Cp^*CH_3). ^{13}C NMR (101 MHz, $CDCl_3$, δ): 155.9 ($C_{carbene}$), 140.5 ($Cp^*CH_2CH_2Ph$), 128.8 ($Cp^*CH_2CH_2Ph$), 128.6 ($Cp^*CH_2CH_2Ph$), 126.5 ($Cp^*CH_2CH_2Ph$), 123.3 ($CH_{backbone}$), 90.4 (Cp^*C), 89.1 (Cp^*C), 87.0 (Cp^*C), 38.7 (NCH_3), 34.6 ($Cp^*CH_2CH_2Ph$), 27.1 ($Cp^*CH_2CH_2Ph$), 9.09 (Cp^*CH_3), 9.07 (Cp^*CH_3). HRMS/ESI+ (m/z): calcd for $C_{22}H_{29}Cl[^{193}Ir]N_2$, 549.1643; found, 549.1625.

Synthesis of ***Ir-15***. Following the general procedure, 1,3-dimethylimidazolium iodide (0.0171 g, 0.0763 mmol), silver(I) oxide (0.0124 g, 0.0534 mmol), and $[(Cp^{*C_6F_5})IrCl_2]_2$ (0.0400 g, 0.0363 mmol) were reacted in dichloromethane to give **Ir-15** (0.0362 g, 77%). ^{1}H NMR (400 MHz, $CDCl_3$, δ): 6.94 (s, 2H, $CH_{backbone}$), 3.96 (s, 6H, NCH_3), 1.72 (dd, J = 1.9, 0.8 Hz, 6H, Cp^*CH_3), 1.63 (s, 6H, Cp^*CH_3). ^{13}C NMR (101 MHz, $CDCl_3$, δ): 152.1 ($C_{carbene}$), 123.7 ($CH_{backbone}$), 97.1 (Cp^*C), 84.7 (Cp^*C), 39.0 (NCH_3), 10.1 (dd, J = 3.6, 1.8 Hz, Cp^*CH_3), 9.8 (Cp^*CH_3). ^{19}F NMR (376 MHz, $CDCl_3$, δ): −124.83 (d, J = 24.2 Hz, 1F, F_{ortho}), −138.22 (d, J = 23.2 Hz, 1F, F_{ortho}), −152.74 (t, J = 21.3 Hz, 1F, F_{para}), −159.52 (td, J = 22.9, 7.6 Hz, 1F, F_{meta}), −162.50 (td, J = 22.6, 8.6 Hz, 1F, F_{meta}). HRMS/ESI+ (m/z): calcd for $C_{20}H_{20}ClF_5[^{193}Ir]N_2$, 611.0864; found, 611.0911.

Antimicrobial Testing. Minimum inhibitory concentrations (MICs) were measured by a broth microdilution of fresh overnight cultures of *Staphylococcus aureus*, methicillin-resistant *Staphylococcus aureus* (MRSA), *Escherichia coli*, *Pseudomonas aeruginosa*, *Candida albicans*, *Aspergillus niger*, *Mycobacterium smegmatis*, *Mycobacterium marinum*, *Mycobacterium abscessus*, *Mycobacterium chelonae*, *Mycobacterium fortuitum* (Type I), *Mycobacterium fortuitum* (Type III), *Mycobacterium avium*, *Mycobacterium intracellulare*, and *Mycobacterium chimaera* according to the Clinical and Laboratory Standards Institute (CLSI) guidelines with 10% brain heart infusion broth (BHIB) containing 0.1% (w/v) dimethyl sulfoxide at an inoculum of 10^5 CFU/mL or Middlebrook 7H9 broth containing 0.5% (w/v) glycerol and 10% (w/v) oleic acid-albumin (*Mycobacterium* spp. strains).[42]

The rhodium and iridium complexes and imidazolium salts were likewise dissolved in the same media, inoculated with 50 μL of a 1000-fold dilution of each mid log-phase microbial culture, and then subjected to a 2-fold dilution series in 96-well microtiter plates before incubation at 30 or 37 °C. After 3 days, the MIC (μg/mL), defined to be the lowest concentration of compound completely inhibiting the appearance of turbidity by eye, was determined and confirmed by absorbance at 540 nm. Control wells containing 50 μL of a 1000-fold dilution of each mid log-phase microbial culture were inoculated with 10% BHIB containing 0.1% (w/v) dimethyl sulfoxide to confirm that 0.1% DMSO alone does not inhibit growth. The MICs reported were converted from units of μg/mL to μM, and all of the MIC values of all compounds screened in this work (in units of μg/mL and μM) are provided in the Supporting Information.

Cytotoxicity Testing. Vero E6 and Calu-3 cells in complete medium were seeded in individual 96-well flat bottom plates until around 80% confluency. Five wells were not seeded as a positive control to determine background values. After confluency was reached, media were decanted from the plate and replaced with media supplemented with **Rh-4** at concentrations of 2.5, 5, 10, 25, and 50 μg/mL in replicates of five. Positive and negative controls received unsupplemented media. Plates were incubated at 37 °C with 5% CO_2 for 24 h. After 24 h, the plates were decanted and the wells were rinsed with media. Fresh media (100 μL) was placed in all of the wells, and the CellTiter 96 AQ_{ueous} One Solution Cell Proliferation Assay (MTS) was used to assess cell viability. CellTiter 96 AQ_{ueous} One Solution Reagent (20 μL) was placed in each well, and plates were incubated at 37 °C for approximately 4 h. After incubation, plates were read on a spectrophotometer at 490 nm to determine absorbance values.

■ ASSOCIATED CONTENT

Supporting Information

The Supporting Information is available free of charge at https://pubs.acs.org/doi/10.1021/acs.organomet.1c00166.

MIC results for all compounds and microbes tested, along with NMR spectra for all novel complexes reported and for the stability studies on **Rh-4** and **Ir-1**, high-resolution mass spectra for **Rh-4** and **Ir-1** as representative examples, and thermal ellipsoid plots for all complexes characterized by single-crystal X-ray diffraction (PDF)

Accession Codes

CCDC 2035763−2035774 contain the supplementary crystallographic data for this paper. These data can be obtained free of charge via www.ccdc.cam.ac.uk/data_request/cif, or by emailing data_request@ccdc.cam.ac.uk, or by contacting The Cambridge Crystallographic Data Centre, 12 Union Road, Cambridge CB2 1EZ, UK; fax: +44 1223 336033.

■ AUTHOR INFORMATION

Corresponding Author

Joseph S. Merola − *Department of Chemistry, Virginia Tech, Blacksburg, Virginia 24061, United States;* orcid.org/0000-0002-1743-1777; Phone: +1 (540)231-4510; Email: jmerola@vt.edu

Authors

Chad M. Bernier − *Department of Chemistry, Virginia Tech, Blacksburg, Virginia 24061, United States;* orcid.org/0000-0002-2829-865X

Christine M. DuChane − *Department of Chemistry, Virginia Tech, Blacksburg, Virginia 24061, United States;* orcid.org/0000-0001-9575-3424

Justin S. Martinez − *Department of Chemistry, Virginia Tech, Blacksburg, Virginia 24061, United States*

Joseph O. Falkinham, III − *Department of Biological Sciences, Virginia Tech, Blacksburg, Virginia 24061, United States*

Complete contact information is available at: https://pubs.acs.org/10.1021/acs.organomet.1c00166

Notes

The authors declare no competing financial interest.

■ ACKNOWLEDGMENTS

The authors thank Myra Williams for performing the antimicrobial testing, Dr. James Weger-Lucarelli and Christina Chuong for conducting the cytotoxicity studies, and Dr. Loren Brown for synthesizing many of the rhodium and iridium Cp^{*R} dimers. We also thank the Virginia Tech Department of Chemistry for funds and supplies. Funding for the Rigaku Oxford Diffraction Synergy diffractometer used in this work was provided by the National Science Foundation (Grant No. 1726077).

■ REFERENCES

(1) Hofer, U. The cost of antimicrobial resistance. *Nat. Rev. Microbiol.* **2019**, *17*, 3−3.

(2) (a) Frei, A.; Zuegg, J.; Elliott, A. G.; Baker, M.; Braese, S.; Brown, C.; Chen, F.; Dowson, C. G.; Dujardin, G.; Jung, N.; King, A. P.; Mansour, A. M.; Massi, M.; Moat, J.; Mohamed, H. A.; Renfrew, A. K.; Rutledge, P. J.; Sadler, P. J.; Todd, M. H.; Willans, C. E.; Wilson, J. J.; Cooper, M. A.; Blaskovich, M. A. T. Metal complexes as a promising source for new antibiotics. *Chem. Sci.* **2020**, *11*, 2627−2639. (b) Frei, A. Metal complexes, an untapped source of antibiotic potential? *Antibiotics* **2020**, *9*, 90.

(3) (a) Mjos, K. D.; Orvig, C. Metallodrugs in medicinal inorganic chemistry. *Chem. Rev.* **2014**, *114*, 4540−4563. (b) Medici, S.; Peana, M.; Nurchi, V. M.; Lachowicz, J. I.; Crisponi, G.; Zoroddu, M. A. Noble metals in medicine: Latest advances. *Coord. Chem. Rev.* **2015**, *284*, 329−350. (c) Regiel-Futyra, A.; Dąbrowski, J. M.; Mazuryk, O.; Śpiewak, K.; Kyzioł, A.; Pucelik, B.; Brindell, M.; Stochel, G. Bioinorganic antimicrobial strategies in the resistance era. *Coord. Chem. Rev.* **2017**, *351*, 76−117. (d) Azharuddin, M.; Zhu, G. H.; Das, D.; Ozgur, E.; Uzun, L.; Turner, A. P. F.; Patra, H. K. A repertoire of biomedical applications of noble metal nanoparticles. *Chem. Commun.* **2019**, *55*, 6964−6996. (e) Nasiri Sovari, S.; Zobi, F. Recent Studies on the Antimicrobial Activity of Transition Metal Complexes of Groups 6−12. *Chemistry (Easton)* **2020**, *2*, 418−452. (f) Claudel, M.; Schwarte, J. V.; Fromm, K. M. New antimicrobial strategies based on metal complexes. *Chemistry (Easton).* **2020**, *2*, 849−899.

(4) Li, F.; Collins, J. G.; Keene, F. R. Ruthenium complexes as antimicrobial agents. *Chem. Soc. Rev.* **2015**, *44*, 2529−2542.

(5) Garoufis, A.; Hadjikakou, S.; Hadjiliadis, N. Palladium coordination compounds as anti-viral, anti-fungal, anti-microbial and anti-tumor agents. *Coord. Chem. Rev.* **2009**, *253*, 1384−1397.

(6) Liang, X.; Luan, S.; Yin, Z.; He, M.; He, C.; Yin, L.; Zou, Y.; Yuan, Z.; Li, L.; Song, X.; Lv, C.; Zhang, W. Recent advances in the medical use of silver complex. *Eur. J. Med. Chem.* **2018**, *157*, 62−80.

(7) Dilruba, S.; Kalayda, G. V. Platinum-based drugs: past, present and future. *Cancer Chemother. Pharmacol.* **2016**, *77*, 1103−1124.

(8) Glisic, B. D.; Djuran, M. I. Gold complexes as antimicrobial agents: an overview of different biological activities in relation to the oxidation state of the gold ion and the ligand structure. *Dalt. Trans.* **2014**, *43*, 5950−5969.

(9) (a) Liu, Z.; Habtemariam, A.; Pizarro, A. M.; Fletcher, S. A.; Kisova, A.; Vrana, O.; Salassa, L.; Bruijnincx, P. C. A.; Clarkson, G. J.; Brabec, V.; Sadler, P. J. Organometallic Half-Sandwich Iridium Anticancer Complexes. *J. Med. Chem.* **2011**, *54*, 3011−3026. (b) Liu, Z.; Habtemariam, A.; Pizarro, A. M.; Clarkson, G. J.; Sadler, P. J. Organometallic Iridium(III) Cyclopentadienyl Anticancer Complexes Containing C,N-Chelating Ligands. *Organometallics* **2011**, *30*, 4702−4710. (c) Almodares, Z.; Lucas, S. J.; Crossley, B. D.; Basri, A. M.; Pask, C. M.; Hebden, A. J.; Phillips, R. M.; McGowan, P. C. Rhodium, iridium, and ruthenium half-sandwich picolinamide complexes as anticancer agents. *Inorg. Chem.* **2014**, *53*, 727−736. (d) Rao, A. B. P.; Palepu, N. R.; Deb, D. K.; Uma, A.; Chiranjeevi, T.; Sarkar, B.; Kaminsky, W.; Rao, K. M. Synthesis, structural, DFT studies and antibacterial evaluation of Cp* rhodium and Cp* iridium complexes using hydrazide based dipyridyl ketone ligand. *Inorg. Chim. Acta* **2016**, *443*, 126−135. (e) Lucas, S. J.; Lord, R. M.; Basri, A. M.; Allison, S. J.; Phillips, R. M.; Blacker, A. J.; McGowan, P. C. Increasing anti-cancer activity with longer tether lengths of group 9 Cp* complexes. *Dalt. Trans.* **2016**, *45*, 6812−6815. (f) Zhang, P.; Sadler, P. J. Advances in the design of organometallic anticancer complexes. *J. Organomet. Chem.* **2017**, *839*, 5−14. (g) Chen, F.; Moat, J.; McFeely, D.; Clarkson, G.; Hands-Portman, I. J.; Furner-Pardoe, J. P.; Harrison, F.; Dowson, C. G.; Sadler, P. J. Biguanide Iridium(III) Complexes with Potent Antimicrobial Activity. *J. Med. Chem.* **2018**, *61*, 7330−7344. (h) Guo, L.; Zhang, H.; Tian, M.; Tian, Z.; Xu, Y.; Yang, Y.; Peng, H.; Liu, P.; Liu, Z. Electronic effects on reactivity and anticancer activity by half-sandwich N,N-chelated iridium(III) complexes. *New J. Chem.* **2018**, *42*, 16183−16192. (i) Lapasam, A.; Banothu, V.; Addepally, U.; Kollipara, M. R. Synthesis, structural and antimicrobial studies of half-sandwich ruthenium, rhodium and iridium complexes containing nitrogen donor Schiff-base ligands. *J. Mol. Struct.* **2019**, *1191*, 314−322. (j) Lapasam, A.; Banothu, V.; Addepally, U.; Kollipara, M. R. Half-sandwich arene ruthenium, rhodium and iridium thiosemicarbazone complexes: synthesis, characterization and biological evaluation. *J. Chem. Sci.* **2020**, *132*, 34. (k) Lapasam, A.; Mawnai, I. L.; Banothu, V.; Kaminsky, W.; Kollipara, M. R. Ruthenium, rhodium and iridium complexes containing pyrimidine based thienyl pyrazoles: Synthesis and antibacterial studies. *J. Organomet. Chem.* **2020**, *911*, 121155. (l) Aboura, W.; Batchelor, L. K.; Garci, A.; Dyson, P. J.; Therrien, B. Reactivity and biological activity of N,N,S-Schiff-base rhodium pentamethylcyclopentadienyl complexes. *Inorg. Chim. Acta* **2020**, *501*, 119265. (m) Mansour, A. M.; Radacki, K. Antimicrobial properties of half-sandwich Ir(III) cyclopentadienyl complexes with pyridylbenzimidazole ligands. *Dalt. Trans.* **2020**, *49*, 4491−4501. (n) Dkhar, L.; Banothu, V.; Kaminsky, W.; Kollipara, M. R. Synthesis of half sandwich platinum group metal complexes containing pyridyl benzothiazole hydrazones: Study of bonding modes and antimicrobial activity. *J. Organomet. Chem.* **2020**, *914*, 121225. (o) Baartzes, N.; Jordaan, A.; Warner, D. F.; Combrinck, J.; Taylor, D.; Chibale, K.; Smith, G. S. Antimicrobial evaluation of neutral and cationic iridium(III) and rhodium(III) aminoquinoline-benzimidazole hybrid complexes. *Eur. J. Med. Chem.* **2020**, *206*, 112694.

(10) Lapasam, A.; Dkhar, L.; Joshi, N.; Poluri, K. M.; Kollipara, M. R. Antimicrobial selectivity of ruthenium, rhodium, and iridium half sandwich complexes containing phenyl hydrazone Schiff base ligands towards B. thuringiensis and P. aeruginosa bacteria. *Inorg. Chim. Acta* **2019**, *484*, 255−263.

(11) Odularu, A. T.; Ajibade, P. A.; Mbese, J. Z.; Oyedeji, O. O. Developments in platinum-group metals as dual antibacterial and anticancer agents. *J. Chem.* **2019**, *2019*, 1−18.

(12) (a) Gupta, R. K.; Pandey, R.; Sharma, G.; Prasad, R.; Koch, B.; Srikrishna, S.; Li, P.-Z.; Xu, Q.; Pandey, D. S. DNA binding and anticancer activity of redox-active heteroleptic piano-stool Ru(II), Rh(III), and Ir(III) complexes containing 4-(2-methoxypyridyl)-phenyldipyrromethene. *Inorg. Chem.* **2013**, *52*, 3687−3698. (b) Liu, Z.; Sadler, P. J. Organoiridium complexes: Anticancer agents and catalysts. *Acc. Chem. Res.* **2014**, *47*, 1174−1185. (c) Liu, Z.; Romero-Canelón, I.; Qamar, B.; Hearn, J. M.; Habtemariam, A.; Barry, N. P. E.; Pizarro, A. M.; Clarkson, G. J.; Sadler, P. J. The potent oxidant anticancer activity of organoiridium catalysts. *Angew. Chem.* **2014**, *126*, 4022−4027. (d) van Rijt, S. H.; Romero-Canelón, I.; Fu, Y.; Shnyder, S. D.; Sadler, P. J. Potent organometallic osmium compounds induce mitochondria-mediated apoptosis and S-phase cell cycle arrest in A549 non-small cell lung cancer cells. *Metallomics* **2014**, *6*, 1014. (e) Jain, N.; Alam, P.; Laskar, I. R.; Panwar, J. 'Aggregation induced phosphorescence' active iridium(III) complexes for integrated sensing and inhibition of bacterial growth in aqueous solution. *RSC Adv.* **2015**, *5*, 61983−61988. (f) Soldevila-Barreda, J. J.; Romero-Canelón, I.; Habtemariam, A.; Sadler, P. J. Transfer hydrogenation catalysis in cells as a new approach to anticancer drug design. *Nat. Commun.* **2015**, *6*, 6582. (g) Wootton, C. A.; Sanchez-Cano, C.; Lopez-Clavijo, A. F.; Shaili, E.; Barrow, M. P.; Sadler, P. J.; O'Connor, P. B. Sequence-dependent attack on peptides by photoactivated platinum anticancer complexes. *Chem. Sci.* **2018**, *9*, 2733−2739. (h) Wootton, C. A.; Millett, A. J.; Lopez-Clavijo, A. F.; Chiu, C. K. C.; Barrow, M. P.; Clarkson, G. J.; Sadler, P. J.; O'Connor, P. B. Structural analysis of peptides modified with organo-iridium complexes, opportunities from multi-mode fragmentation. *Analyst* **2019**, *144*, 1575−1581.

(13) (a) Hopkinson, M. N.; Richter, C.; Schedler, M.; Glorius, F. An overview of N-heterocyclic carbenes. *Nature* **2014**, *510*, 485−496. (b) Hindi, K. M.; Panzner, M. J.; Tessier, C. A.; Cannon, C. L.; Youngs, W. J. The medicinal applications of imidazolium carbene-metal complexes. *Chem. Rev.* **2009**, *109*, 3859−3884. (c) Oehninger, L.; Rubbiani, R.; Ott, I. N-Heterocyclic carbene metal complexes in medicinal chemistry. *Dalt. Trans.* **2013**, *42*, 3269−3284. (d) Liu, W.; Gust, R. Metal N-heterocyclic carbene complexes as potential antitumor metallodrugs. *Chem. Soc. Rev.* **2013**, *42*, 755−773. (e) Patil, S. A.; Patil, S. A.; Patil, R.; Keri, R. S.; Budagumpi, S.; Balakrishna, G. R.; Tacke, M. N-Heterocyclic carbene metal complexes as bio-organometallic antimicrobial and anticancer drugs.

https://doi.org/10.1021/acs.organomet.1c00166
Organometallics 2021, 40, 1670−1681

Future Med. Chem. **2015**, *7*, 1305−1333. (f) Liu, W.; Gust, R. Update on metal N-heterocyclic carbene complexes as potential anti-tumor metallodrugs. *Coord. Chem. Rev.* **2016**, *329*, 191−213. (g) Ott, I.; Sadler, P. J.; van Eldik, R. *Adv. Inorg. Chem.* **2020**, *75*, 121−148.

(14) (a) Ray, S.; Mohan, R.; Singh, J. K.; Samantaray, M. K.; Shaikh, M. M.; Panda, D.; Ghosh, P. Anticancer and antimicrobial metallopharmaceutical agents based on palladium, gold, and silver N-heterocyclic carbene complexes. *J. Am. Chem. Soc.* **2007**, *129*, 15042−15053. (b) Kascatan-Nebioglu, A.; Panzner, M. J.; Tessier, C. A.; Cannon, C. L.; Youngs, W. J. N-Heterocyclic carbene−silver complexes: A new class of antibiotics. *Coord. Chem. Rev.* **2007**, *251*, 884−895. (c) Johnson, N. A.; Southerland, M. R.; Youngs, W. J. Recent developments in the medicinal applications of silver-NHC complexes and imidazolium salts. *Molecules* **2017**, *22*, 1263. (d) Mora, M.; Gimeno, M. C.; Visbal, R. Recent advances in gold−NHC complexes with biological properties. *Chem. Soc. Rev.* **2019**, *48*, 447−462. (e) Hussaini, S. Y.; Haque, R. A.; Razali, M. R. Recent progress in silver(I)-, gold(I)/(III)- and palladium(II)-N-heterocyclic carbene complexes: A review towards biological perspectives. *J. Organomet. Chem.* **2019**, *882*, 96−111.

(15) (a) Truong, D.; Sullivan, M. P.; Tong, K. K. H.; Steel, T. R.; Prause, A.; Lovett, J. H.; Andersen, J. W.; Jamieson, S. M.; Harris, H. H.; Ott, I.; Weekley, C. M.; Hummitzsch, K.; Söhnel, T.; Hanif, M.; Metzler-Nolte, N.; Goldstone, D. C.; Hartinger, C. G. Potent inhibition of thioredoxin reductase by the Rh derivatives of anticancer M(arene/Cp*)(NHC)Cl2 complexes. *Inorg. Chem.* **2020**, *59*, 3281−3289. (b) Wang, C.; Liu, J.; Tian, Z.; Tian, M.; Tian, L.; Zhao, W.; Liu, Z. Half-sandwich iridium N-heterocyclic carbene anticancer complexes. *Dalt. Trans.* **2017**, *46*, 6870−6883. (c) Yang, Y.; Guo, L.; Tian, Z.; Gong, Y.; Zheng, H.; Zhang, S.; Xu, Z.; Ge, X.; Liu, Z. Novel and versatile imine-N-Heterocyclic carbene half-sandwich iridium(III) complexes as lysosome-targeted anticancer agents. *Inorg. Chem.* **2018**, *57*, 11087−11098. (d) Lord, R. M.; McGowan, P. C. Organometallic iridium arene compounds: The effects of C -donor ligands on anticancer activity. *Chem. Lett.* **2019**, *48*, 916−924. (e) Yang, Y.; Guo, L.; Ge, X.; Shi, S.; Gong, Y.; Xu, Z.; Zheng, X.; Liu, Z. Structure-activity relationships for highly potent half-sandwich organoiridium-(III) anticancer complexes with C****N-chelated ligands. *J. Inorg. Biochem.* **2019**, *191*, 1−7.

(16) (a) Hackenberg, F.; Lally, G.; Müller-Bunz, H.; Paradisi, F.; Quaglia, D.; Streciwilk, W.; Tacke, M. Synthesis and biological evaluation of N-heterocyclic carbene−silver(I) acetate complexes derived from 4,5-ditolyl-imidazole. *Inorg. Chim. Acta* **2013**, *395*, 135−144. (b) Haque, R. A.; Ghdhayeb, M. Z.; Budagumpi, S.; Khadeer Ahamed, M. B.; Abdul Majid, A. M. S. Synthesis, crystal structures, and in vitro anticancer properties of new N-heterocyclic carbene (NHC) silver(I)- and gold(I)/(III)-complexes: a rare example of silver(I)−NHC complex involved in redox transmetallation. *RSC Adv.* **2016**, *6*, 60407−60421. (c) Kascatan-Nebioglu, A.; Melaiye, A.; Hindi, K.; Durmus, S.; Panzner, M. J.; Hogue, L. A.; Mallett, R. J.; Hovis, C. E.; Coughenour, M.; Crosby, S. D.; Milsted, A.; Ely, D. L.; Tessier, C. A.; Cannon, C. L.; Youngs, W. J. Synthesis from caffeine of a mixed N-heterocyclic carbene-silver acetate complex active against resistant respiratory pathogens. *J. Med. Chem.* **2006**, *49*, 6811−6818. (d) Schmidt, C.; Karge, B.; Misgeld, R.; Prokop, A.; Franke, R.; Brönstrup, M.; Ott, I. Gold(I) NHC complexes: Antiproliferative activity, cellular uptake, inhibition of mammalian and bacterial thioredoxin reductases, and gram-positive directed antibacterial effects. *Chem. - Eur. J.* **2017**, *23*, 1869−1880.

(17) (a) Cetinkaya, B.; Cetinkaya, E.; Küçükbay, H.; Durmaz, R. Antimicrobial activity of carbene complexes of rhodium(I) and ruthenium(II). *Arzneimittelforschung* **1996**, *46*, 821−823. (b) Simpson, P. V.; Schmidt, C.; Ott, I.; Bruhn, H.; Schatzschneider, U. Synthesis, cellular uptake and biological Activity against pathogenic micro-organisms and cancer cells of rhodium and iridium N-heterocyclic carbene complexes bearing charged substituents. *Eur. J. Inorg. Chem.* **2013**, *2013*, 5547−5554. (c) Streciwilk, W.; Terenzi, A.; Cheng, X.; Hager, L.; Dabiri, Y.; Prochnow, P.; Bandow, J. E.; Wölfl, S.; Keppler, B. K.; Ott, I. Fluorescent organometallic rhodium(I) and ruthenium-(II) metallodrugs with 4-ethylthio-1,8-naphthalimide ligands: Anti-proliferative effects, cellular uptake and DNA-interaction. *Eur. J. Med. Chem.* **2018**, *156*, 148−161.

(18) Karpin, G. W.; Merola, J. S.; Falkinham, J. O. Transition Metal−α-Amino Acid Complexes with Antibiotic Activity against Mycobacterium spp. *Antimicrob. Agents Chemother.* **2013**, *57*, 3434−3436.

(19) Karpin, G. W.; Morris, D. M.; Ngo, M. T.; Merola, J. S.; Falkinham, J. O., III Transition metal diamine complexes with antimicrobial activity against Staphylococcus aureus and methicillin-resistant S. aureus (MRSA). *MedChemComm* **2015**, *6*, 1471−1478.

(20) DuChane, C. M.; Brown, L. C.; Dozier, V. S.; Merola, J. S. Synthesis, Characterization, and Antimicrobial Activity of Rh III and Ir III β-Diketonato Piano-Stool Compounds. *Organometallics* **2018**, *37*, 530−538.

(21) DuChane, C. M.; Karpin, G. W.; Ehrich, M.; Falkinham, J. O.; Merola, J. S. Iridium piano stool complexes with activity against S. aureus and MRSA: it is past time to truly think outside of the box. *MedChemComm* **2019**, *10*, 1391−1398.

(22) Xiao, X.-Q.; Jin, G.-X. Half-sandwich rhodium complexes containing both N-heterocyclic carbene and ortho-carborane-1,2-dithiolate ligands. *J. Organomet. Chem.* **2008**, *693*, 316−320.

(23) Xiao, X.-Q.; Jin, G.-X. Functionalized N-heterocyclic carbene iridium complexes: Synthesis, structure and addition polymerization of norbornene. *J. Organomet. Chem.* **2008**, *693*, 3363−3368.

(24) Tanabe, Y.; Hanasaka, F.; Fujita, K.-i.; Yamaguchi, R. Scope and Mechanistic Studies of Intramolecular Aliphatic C-H Bond Activation of N-Heterocyclic Carbene Iridium Complexes §. *Organometallics* **2007**, *26*, 4618−4626.

(25) Prinz, M.; Grosche, M.; Herdtweck, E.; Herrmann, W. A. Unsymmetrically Substituted Iridium(III)-Carbene Complexes by a CH-Activation Process. *Organometallics* **2000**, *19*, 1692−1694.

(26) Meredith, J. M.; Robinson, R.; Goldberg, K. I.; Kaminsky, W.; Heinekey, D. M. C−H Bond Activation by Cationic Iridium(III) NHC Complexes: A Combined Experimental and Computational Study. *Organometallics* **2012**, *31*, 1879−1887.

(27) (a) Tapu, D.; Dixon, D. A.; Roe, C. 13C NMR spectroscopy of "Arduengo-type" carbenes and their derivatives. *Chem. Rev.* **2009**, *109*, 3385−3407. (b) Huynh, H. V. Electronic properties of N-heterocyclic carbenes and their experimental determination. *Chem. Rev.* **2018**, *118*, 9457−9492.

(28) Huynh, H. V. *The Organometallic Chemistry of N-heterocyclic Carbenes*; Wiley: Chichester, U.K., 2017; Chapter 7, pp 220−262. DOI: 10.1002/9781118698785.ch7.

(29) da Costa, A. P.; Sanaú, M.; Peris, E.; Royo, B. Easy preparation of Cp*-functionalized N-heterocyclic carbenes and their coordination to rhodium and iridium. *Dalt. Trans.* **2009**, 6960−6966.

(30) Groom, C. R.; Bruno, I. J.; Lightfoot, M. P.; Ward, S. C. The Cambridge Structural Database. *Acta Crystallogr., Sect. B: Struct. Sci., Cryst. Eng. Mater.* **2016**, *72*, 171−179.

(31) (a) Gradert, C.; Krahmer, J.; Sönnichsen, F.; Näther, C.; Tuczek, F. Molybdenum(0)−carbonyl complexes supported by mixed benzimidazol-2-ylidene/phosphine ligands: Influence of benzannulation on the donor properties of the NHC groups. *J. Organomet. Chem.* **2014**, *770*, 61−68. (b) Karabıyık, H.; Yigit, B.; Yigit, M.; Ozdemir, I.; Karabiyik, H. Enhanced π-back-donation resulting in the trans labilization of a pyridine ligand in an N-heterocyclic carbene (NHC) Pd II precatalyst: a case study. *Acta Crystallogr., Sect. C: Struct. Chem.* **2019**, *75*, 941−950.

(32) Gardner, S.; Kawamoto, T.; Curran, D. P. Synthesis of 1,3-Dialkylimidazol-2-ylidene Boranes from 1,3-Dialkylimidazolium Iodides and Sodium Borohydride. *J. Org. Chem.* **2015**, *80*, 9794−9797.

(33) Huang, S.; Qi, X.; Liu, T.; Wang, K.; Zhang, W.; Li, J.; Zhang, Q. Towards Safer Rocket Fuels: Hypergolic Imidazolylidene-Borane Compounds as Replacements for Hydrazine Derivatives. *Chem. - Eur. J.* **2016**, *22*, 10187−10193.

(34) Roberts, G. M.; Pierce, P. J.; Woo, L. K. Palladium Complexes with N-Heterocyclic Carbene Ligands As Catalysts for the

Alkoxycarbonylation of Olefins. *Organometallics* **2013**, *32*, 2033−2036.
(35) Brown, L. C.; Ressegue, E.; Merola, J. S. Rapid Access to Derivatized, Dimeric, Ring-Substituted Dichloro(cyclopentadienyl)-rhodium(III) and Iridium(III) Complexes. *Organometallics* **2016**, *35*, 4014−4022.
(36) *CrysAlisPRO*; Oxford Diffraction/Agilent Technologies UK Ltd: Yarnton, England.
(37) Sheldrick, G. M. SHELXT − Integrated space-group and crystal-structure determination. *Acta Crystallogr., Sect. A: Found. Adv.* **2015**, *71*, 3−8.
(38) Sheldrick, G. M. Crystal structure refinement with SHELXL. *Acta Crystallogr., Sect. C: Struct. Chem.* **2015**, *71*, 3−8.
(39) Dolomanov, O. V.; Bourhis, L. J.; Gildea, R. J.; Howard, J. A. K.; Puschmann, H. OLEX2: a complete structure solution, refinement and analysis program. *J. Appl. Crystallogr.* **2009**, *42*, 339−341.
(40) Bruno, I. J.; Cole, J. C.; Edgington, P. R.; Kessler, M.; Macrae, C. F.; McCabe, P.; Pearson, J.; Taylor, R. New software for searching the Cambridge Structural Database and visualizing crystal structures. *Acta Crystallogr., Sect. B: Struct. Sci.* **2002**, *58*, 389−397.
(41) (a) Macrae, C. F.; Edgington, P. R.; McCabe, P.; Pidcock, E.; Shields, G. P.; Taylor, R.; Towler, M.; van de Streek, J. Mercury: visualization and analysis of crystal structures. *J. Appl. Crystallogr.* **2006**, *39*, 453−457. (b) Macrae, C. F.; Bruno, I. J.; Chisholm, J. A.; Edgington, P. R.; McCabe, P.; Pidcock, E.; Rodriguez-Monge, L.; Taylor, R.; van de Streek, J.; Wood, P. A. Mercury CSD 2.0 − new features for the visualization and investigation of crystal structures. *J. Appl. Crystallogr.* **2008**, *41*, 466−470.
(42) Maisuria, B. B.; Actis, M. L.; Hardrict, S. N.; Falkinham, J. O.; Cole, M. F.; Cihlar, R. L.; Peters, S. M.; Macri, R. V.; Sugandhi, E. W.; Williams, A. A.; Poppe, M. A.; Esker, A. R.; Gandour, R. D. Comparing micellar, hemolytic, and antibacterial properties of di- and tricarboxyl dendritic amphiphiles. *Bioorg. Med. Chem.* **2011**, *19*, 2918−2926.

https://doi.org/10.1021/acs.organomet.1c00166
Organometallics 2021, 40, 1670−1681